

Critical heat current for operating an entanglement engine

Shishir Khandelwal, Nicolas Palazzo, Nicolas Brunner,
Géraldine Haack

Department of Applied Physics, University of Geneva, Chemin de Pinchat 22, 1227
Carouge, Genève, Switzerland

Abstract. Autonomous entanglement engines have recently been proposed to generate steady-state bipartite and multipartite entanglement exploiting only incoherent interactions with thermal baths at different temperatures. In this work, for a two-qubit entanglement engine in the steady-state regime, we derive an analytical relation between the heat flow and entanglement by showing there exists a critical heat current for successful operation of the engine, i.e. a cut-off above which entanglement is present. The heat current can thus be seen as a witness to the presence of entanglement between the qubits. We further show that while energy detuning and tunnelling in general reduce the amount of entanglement, both effects can compensate each other for specific values.

1. Introduction

Autonomous quantum thermal machines - ones that function without external sources of coherence or control, have gathered considerable interest in recent years [1–3]. There are two primary reasons for this interest. Firstly, the elimination of the requirement of classical control may allow one to explore what is truly “quantum” in quantum thermal machines. Secondly, the thermodynamic cost of classical control can render the thermal machine useless for all practical purposes. Many recent proposals involve autonomous quantum thermal machines performing thermodynamical tasks associated with classical thermal machines such as work extraction and refrigeration [4–7], thermometry [8], clock realization [9], and explore how quantum features can be advantageous (see for example [10, 11]). In practise, these ideas can be implemented by exploiting the quantisation of energy levels in nanostructures [12–18], single-particle quantum coherence [19, 20], many-body effects [21–23] and unconventional materials or phases of matter [24–27].

Remarkably, another type of autonomous thermal machines has recently been put forward, machines that exploit thermal resources to generate bipartite entanglement between two qubits [14]. This idea has then been further extended to generate multipartite entangled states (for example Bell, GHZ or W-states) [28, 29] or using non-thermal baths [30]. They have two key features. Firstly, they provide a simple

and exciting platform to study the intersection of quantum information and quantum thermodynamics, which is a growing field of study [31]. Secondly, and importantly, quantum entanglement lacking a classical counterpart, they involve a truly quantum effect in the thermodynamic setting.

In Ref. [14], it was shown that a heat current is necessary to generate entanglement between two qubits in the steady-state. In this work, we go beyond by establishing an exact relation between heat current and entanglement generation, i.e we derive a critical heat current that must be satisfied for the entanglement engine to function successfully. This result can be seen as a heat current based entanglement witness. In the presence of energy detuning, we provide an analytical expression of this critical heat current. We also study the effects of tunnelling; our numerical results show that the qubits can be entangled in the steady-state for a large range of relevant parameters in experiments.

2. System and steady-state solution

We consider two interacting qubits with energy gaps ε_h and ε_c (figure 1) and let them be coupled to distinct thermal baths at temperatures T_h and T_c with $T_h > T_c$, respectively. The qubits are referred to as *hot* and *cold* throughout. Let the Hamiltonian of the system be

$$H = H_S + H_{\text{int}} + H_B + H_{\text{SB}} \quad (1)$$

where H_S is the Hamiltonian of the two qubits, H_{int} is the interaction between them, H_B is the Hamiltonian of the two baths and H_{SB} is the interaction between the qubits and the baths. Explicitly, they take the form:

$$\begin{aligned} H_S &= \sum_{j \in \{h,c\}} \varepsilon_j \sigma_+^{(j)} \sigma_-^{(j)} & H_{\text{int}} &= g \left(\sigma_+^{(h)} \sigma_-^{(c)} + \sigma_-^{(h)} \sigma_+^{(c)} \right) \\ H_B &= \sum_{j \in \{h,c\}} \omega_j c_j^\dagger c_j & H_{\text{SB}} &= \sum_{j \in \{h,c\}} \left(\alpha_j \sigma_-^{(j)} c_j^\dagger + \alpha_j^* \sigma_+^{(j)} c_j \right), \end{aligned} \quad (2)$$

with the raising and lowering operators $\sigma_+ := |1\rangle\langle 0|$ and $\sigma_- := |0\rangle\langle 1|$, with $|1\rangle := (1, 0)^T$ and $|0\rangle := (0, 1)^T$. α_j s characterise the interaction strength between the qubits with their respective baths. The creation and annihilation operators c_j and c_j^\dagger , for bosonic baths, satisfy the canonical commutation relation, $[c_i, c_j^\dagger] = \mathbf{1} \delta_{ij}$.

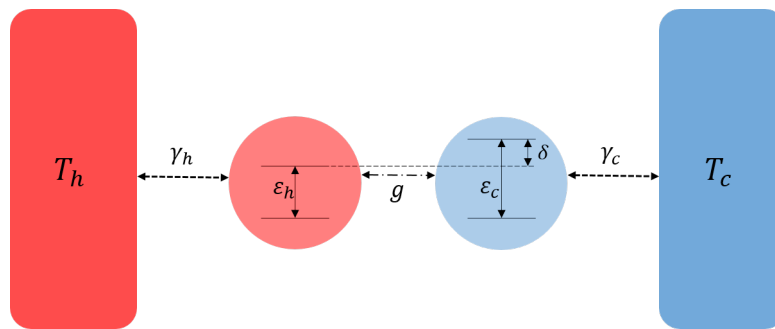


Figure 1: Sketch of an autonomous two-qubit entanglement engine: two qubits are coupled to distinct thermal baths, weakly interacting with each other with strength g . Qubit j with energy gap ε_j is coupled to bath at temperature T_j with strength γ_j . Energy detuning between the two qubits is labelled $\delta = \varepsilon_c - \varepsilon_h$.

Born-Markov and rotating-wave approximations allow the evolution of the two-qubit system to be described by a Lindblad master equation [34–36]. To describe the evolution of interacting systems with master equations, one may take the *local* approach in which the environment couples locally with subsystems, or the *global* approach in which the environment couples to global degrees of freedom of the system. The choice depends on the coupling strength g versus the coupling strengths to the baths γ_j with respect to the energies of the qubits and has been discussed at length in [37–39]. In our model, the use of a local master equation is justified if $g \ll \varepsilon$. This approximation is also of course, in addition to the limit of weak coupling between the system and baths, $\gamma_j \ll \varepsilon$. Furthermore, since we consider non-degenerate qubits in our analysis, we must impose that the detuning δ be much smaller than the gaps themselves, $\delta \ll \varepsilon_{h,c}$. The evolution of the two qubits is then given by (note that we set $\hbar = k_B = 1$ throughout)

$$\dot{\rho}(t) = -i[H_S + H_{\text{int}}, \rho(t)] + \sum_{j \in \{h,c\}} \gamma_j^+ \mathcal{D}[\sigma_+^{(j)}] \rho(t) + \gamma_j^- \mathcal{D}[\sigma_-^{(j)}] \rho(t) \quad (3)$$

with the dissipators $\mathcal{D}[A] \cdot := A \cdot A^\dagger - \{A^\dagger A, \cdot\}/2$, and the exact coupling rates are determined by the underlying statistics of the baths. Specifically, in the case of coupling to bosonic baths,

$$\gamma_j^+ = \gamma_j n_B^{(j)} \quad \text{and} \quad \gamma_j^- = \gamma_j (1 + n_B^{(j)}), \quad j \in \{h, c\}. \quad (4)$$

The bare rates are given by $\gamma_j(\varepsilon) = 2\pi|\alpha_j|^2$, where α_j s come from the system-bath Hamiltonian H_{SB} in (2). The Bose-Einstein distribution is $n_B^{(j)} = 1/(e^{\beta_j \varepsilon_j} - 1)$ with the inverse temperature $\beta_j = 1/T_j$. To solve the Lindblad equation (3) for the steady-state, we recast it as a matrix differential equation for the vectorised state $\mathbf{p}(t)$ of the density operator $\rho(t)$.

$$\rho(t) \longleftrightarrow \mathbf{p}(t), \quad \dot{\rho}(t) = \mathcal{L}\rho(t) \longleftrightarrow \dot{\mathbf{p}}(t) = M\mathbf{p}(t) + \mathbf{b} \quad (5)$$

M is a 15×16 matrix and \mathbf{b} is a 15×1 vector; see appendix A for the exact expressions. The steady-state solution \mathbf{p}_{ss} satisfies $\dot{\mathbf{p}}_{\text{ss}}(t) = 0$, which using (20) gives us $\mathbf{p}_{\text{ss}} = -M^{-1}\mathbf{b}$. The form of the interaction Hamiltonian H_{int} imposes that only two of the off-diagonal elements in the density matrix $\rho(t)$ are non-zero. In the computational basis of the two qubits $\{|11\rangle, |10\rangle, |01\rangle, |00\rangle\}$, the steady-state density matrix, ρ_{ss} is given by

$$\rho_{\text{ss}} = \begin{pmatrix} r_1 & 0 & 0 & 0 \\ 0 & r_2 & c & 0 \\ 0 & c^* & r_3 & 0 \\ 0 & 0 & 0 & r_4 \end{pmatrix}. \quad (6)$$

The steady-state populations are given by

$$\begin{aligned} r_1 &= \frac{4g^2(\gamma_h^+ + \gamma_c^+)^2 + \gamma_h^+ \gamma_c^+ (\Gamma^2 + 4\delta^2)}{\chi} & r_2 &= \frac{4g^2(\gamma_h^- + \gamma_c^-)(\gamma_h^+ + \gamma_c^+) + \gamma_h^+ \gamma_c^- (\Gamma^2 + 4\delta^2)}{\chi} \\ r_3 &= \frac{4g^2(\gamma_h^- + \gamma_c^-)(\gamma_h^+ + \gamma_c^+) + \gamma_h^- \gamma_c^+ (\Gamma^2 + 4\delta^2)}{\chi} & r_4 &= \frac{4g^2(\gamma_h^- + \gamma_c^-)^2 + \gamma_h^- \gamma_c^- (\Gamma^2 + 4\delta^2)}{\chi}, \end{aligned} \quad (7)$$

and the coherence (off-diagonal term) c is given by

$$c = \frac{2g(\gamma_h^+ \gamma_c^- - \gamma_h^- \gamma_c^+) (i\Gamma - 2\delta)}{\chi}. \quad (8)$$

For convenience, we have introduced the following notation

$$\begin{aligned} \chi &:= (4g^2 + \Gamma_h \Gamma_c) \Gamma^2 + 4\delta^2 \Gamma_h \Gamma_c \\ \Gamma &:= (\gamma_h^- + \gamma_h^+ + \gamma_c^- + \gamma_c^+) \\ \Gamma_j &:= (\gamma_j^- + \gamma_j^+). \end{aligned} \quad (9)$$

As expected, in the case where the coupling g between the qubits is set to zero, the coherences vanish, and when there is no detuning between qubits, they are purely imaginary, in agreement with the previous study in [14]. It is also easy to see that there are no coherences in the reduced steady-states of the two qubits. It is important to note that while the presence of coherence c is essential for the two qubits to be entangled, it is not sufficient to guarantee it. The precise condition on c for the state to be entangled is given in section 4.1.

3. Steady-state heat current

In our master equation approach, the heat flow Q_j from the bath j to qubit j at time t is given by [40, 41]

$$Q_j(t) = \text{Tr} \left[H_S \left(\gamma_j^+ \mathcal{D}_j \left[\sigma_+^{(j)} \right] + \gamma_j^- \mathcal{D}_j \left[\sigma_-^{(j)} \right] \right) \rho(t) \right]. \quad (10)$$

The First Law of thermodynamics [40, 41] imposes that the sum of heat flows from the hot and cold baths must sum to zero, $\sum_{j \in \{c, h\}} Q_j = 0$. Note that we follow the

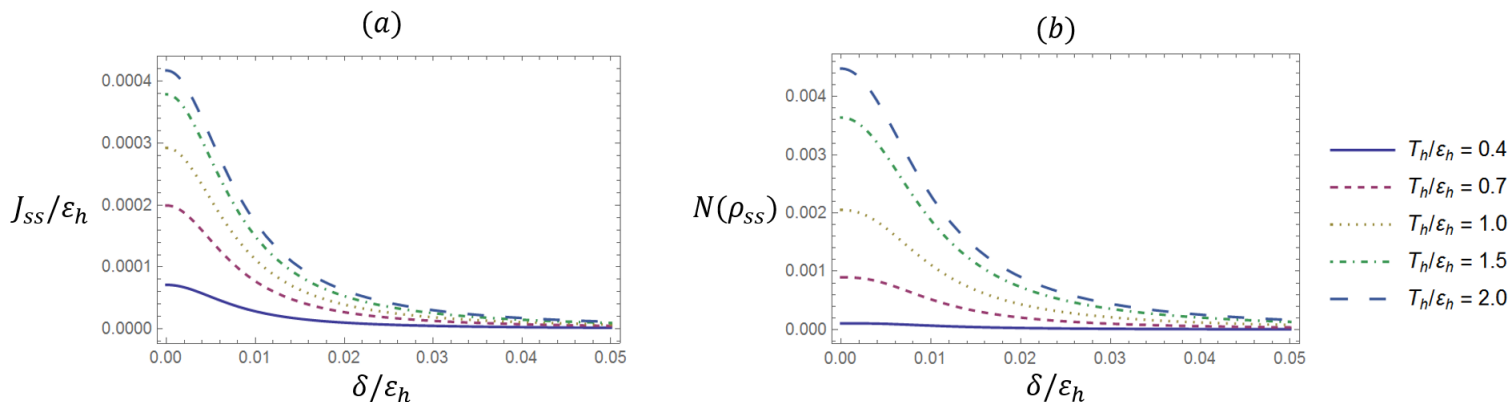


Figure 2: Steady-state (a) heat current J_{ss}/ϵ_h and (b) negativity $N(\rho_{ss})$, as functions of δ/ϵ_h , for different values of T_h/ϵ_h , with $T_c/\epsilon_h = 0.1$, $g = 1.6 \times 10^{-3}$, $\gamma_h = 10^{-3}$ and $\gamma_c = 1.1 \times 10^{-2}$. $\epsilon_h = 1$ is set constant.

convention in which heat flow from a bath to a qubit is positive, so Q_c takes a negative numerical value, while Q_h takes a positive value. Inserting the steady-state solution (6), we find the following expression for the steady-state heat current J_{ss} from the hot bath to the hot qubit

$$\begin{aligned} J_{ss} &:= Q_h^{ss} - Q_c^{ss} \\ &= \frac{8g^2(\gamma_h^+ \gamma_c^- - \gamma_h^- \gamma_c^+)}{\chi} (\epsilon_h \Gamma_c + \epsilon_c \Gamma_h). \end{aligned} \quad (11)$$

The heat current is expected to be of the first-order in the couplings (γ_j and g). For this to be true, the above mentioned condition $\delta \ll \epsilon$ is essential. Taking the underlying bath (Bose-Einstein) statistics into account in $\gamma_h^- \gamma_c^+ - \gamma_h^+ \gamma_c^-$, one finds that the steady-state heat current is proportional to the difference in the distributions of the two baths taken at the energy of each qubit

$$J_{ss} = \frac{8g^2}{\chi} \gamma_h \gamma_c (\epsilon_h \Gamma_c + \epsilon_c \Gamma_h) \left(n_B^{(h)} - n_B^{(c)} \right). \quad (12)$$

This expression may remind the reader of the Landauer-Büttiker form of the heat current [42–45], with the energy window for excitations being set by the energy gap of each qubit. Indeed, in the Markovian limit, excitation tunnelling only takes place at resonance (i.e when the excitation frequencies are equal to the energy gaps of the qubits). In figure 2 (a), we show the variation of heat current J_{ss} , with the detuning between energy gaps δ . There is a reduction in heat current for even small values of detuning that we considered. Furthermore, as expected, the heat currents increase with increase in T_h , with T_c set constant.

3.1. Heat current and coherence

Interestingly, there is a similarity in the expressions for the steady-state heat current J_{ss} and coherence c . Comparing (8) and (11), we can write

$$c = \frac{J_{\text{ss}} (i\Gamma - 2\delta)}{4g (\varepsilon_h \Gamma_c + \varepsilon_c \Gamma_h)}, \quad (13)$$

which makes it clear that the conditions for heat current and coherence being zero are the same. These conditions are also different from simply having decoupled qubits ($g = 0$), in which case the reduced states of the qubits are thermal with the temperatures of their corresponding baths. Therefore the presence of coherence is a signature of the flow of heat and vice-versa.

4. Quantifying steady-state entanglement

To characterise entanglement, we use the entanglement measure referred to as negativity [46, 47]. For an arbitrary state of two qubits $\rho \in \mathcal{S}(\mathcal{H}_h \otimes \mathcal{H}_c)$, the negativity, $N(\rho)$ is defined as

$$N(\rho) := \sum_{\lambda_i < 0} |\lambda_i|, \quad (14)$$

where λ_i s are the eigenvalues of the partial transpose of the density matrix with respect to the one of the qubits. It is simple to see that $N(\rho) = 0$ for a separable state and $N(\rho) = 1/2$ for a Bell state. Using the steady-state solution (6), a straightforward calculation gives

$$N(\rho_{\text{ss}}) = \max \{0, n(\rho_{\text{ss}})\}, \quad (15)$$

where

$$n(\rho_{\text{ss}}) = \frac{1}{2} \left(\sqrt{4|c|^2 + (r_1 - r_4)^2} - (r_1 + r_4) \right). \quad (16)$$

The above equation comes from the fact that only one of the eigenvalues of the partial transpose can be negative in our setup; more details can be found in appendix B. Upon inserting the steady-state solution (7) and (8) in (16), we find the following explicit expression for negativity,

$$n(\rho_{\text{ss}}) = \frac{1}{2\chi} \left[-4g^2 A - B (4\delta^2 + \Gamma^2) + \sqrt{16g^4 (\gamma_h + \gamma_c)^2 \Gamma^2 + 8g^2 C (4\delta^2 + \Gamma^2) + D (4\delta^2 + \Gamma^2)^2} \right], \quad (17)$$

where

$$A = [\gamma_h^2 + \gamma_c^2 + 2(\gamma_h^+ + \gamma_c^-)(\gamma_h^- + \gamma_c^+)],$$

$$B = \gamma_h^- \gamma_c^- + \gamma_h^+ \gamma_c^+,$$

$$C = \gamma_h^+ \gamma_c^+ \left((\gamma_h^+)^2 + (\gamma_c^+)^2 \right) + \gamma_h^- \gamma_c^- \left((\gamma_h^-)^2 + (\gamma_c^-)^2 \right) + 2 \left((\gamma_h^-)^2 + (\gamma_h^+)^2 \right) \left((\gamma_c^-)^2 + (\gamma_c^+)^2 \right),$$

$$- (\gamma_h^- \gamma_h^+ + \gamma_c^- \gamma_c^+) (\gamma_h^- \gamma_c^+ + \gamma_h^+ \gamma_c^-) - 8 \gamma_h^- \gamma_h^+ \gamma_c^- \gamma_c^+,$$

and

$$D = (\gamma_h^- \gamma_c^- - \gamma_h^+ \gamma_c^+)^2.$$

In contrast to the heat current J_{ss} (11), the above expressions do not neatly simplify in terms of the difference between the distributions of the two baths. In figure 2 (b), we show the variation of negativity with detuning in the energy gaps. The plots clearly show reduction in the negativity even for a small amount (5%) of non-degeneracy among the qubits. Furthermore, there is an increase in the steady-state negativity with increase in T_h . These observations are in direct correspondence with the variation of heat current with detuning that was presented above.

4.1. Critical heat current

For the presence of non-zero steady-state entanglement between the two qubits, looking at (16), it is simple to see that the state must satisfy $|c|^2 > r_1 r_4$, which is of course equivalent to the Peres-Horodecki criterion [48, 49]. Interestingly, the populations r_2 and r_3 do not appear in this bound, despite the presence of coherence in their subspace. One way to see this is that the condition $r_2 r_3 > |c|^2$ is satisfied implicitly due to the positivity of the density matrix ρ_{ss} (which is true because Lindbladian evolution is Completely Positive and Trace Preserving (CPTP)). This condition directly leads us to a lower bound on the heat current required to generate non-zero steady-state entanglement via (13).

$$J_{\text{ss}} > \sqrt{\frac{16g^2 r_1 r_4}{\Gamma^2 + 4\delta^2}} (\varepsilon_h \Gamma_c + \varepsilon_c \Gamma_h)^2 := J_c \quad (18)$$

The above lower bound can be understood as follows. For given decay rates, temperatures and energy gaps in the two-qubit thermal machine, there exists a minimum amount of steady-state heat current required for entanglement to be present. Therefore, a finite steady-state heat current is a necessary but not a sufficient condition for entanglement. It leads us to define a *critical* steady-state heat current J_c , a cut-off value of heat current needed to form steady-state entanglement between the two qubits. Alternatively, one may regard the quantity J_{ss}/J_c as a heat current based entanglement witness, as the two qubits are entangled in the steady-state whenever $J_{\text{ss}}/J_c > 1$.

Figure 3 demonstrates the utility of the above analysis. In figure 3 (a), we compare the variation of J_{ss}/J_c and the steady-state negativity $N(\rho_{\text{ss}})$ with the detuning. We see that there is monotonic decrease in J_{ss}/J_c for the considered range of detuning. Observe that the negativity starts from a non-zero value and declines to zero for a particular value of detuning. This is the same value that makes $J_{\text{ss}}/J_c = 1$. Therefore, the lower bound on the heat current allows us to obtain a numerical upper bound on the detuning to have non-zero steady-state entanglement. The analysis is of course only valid in the

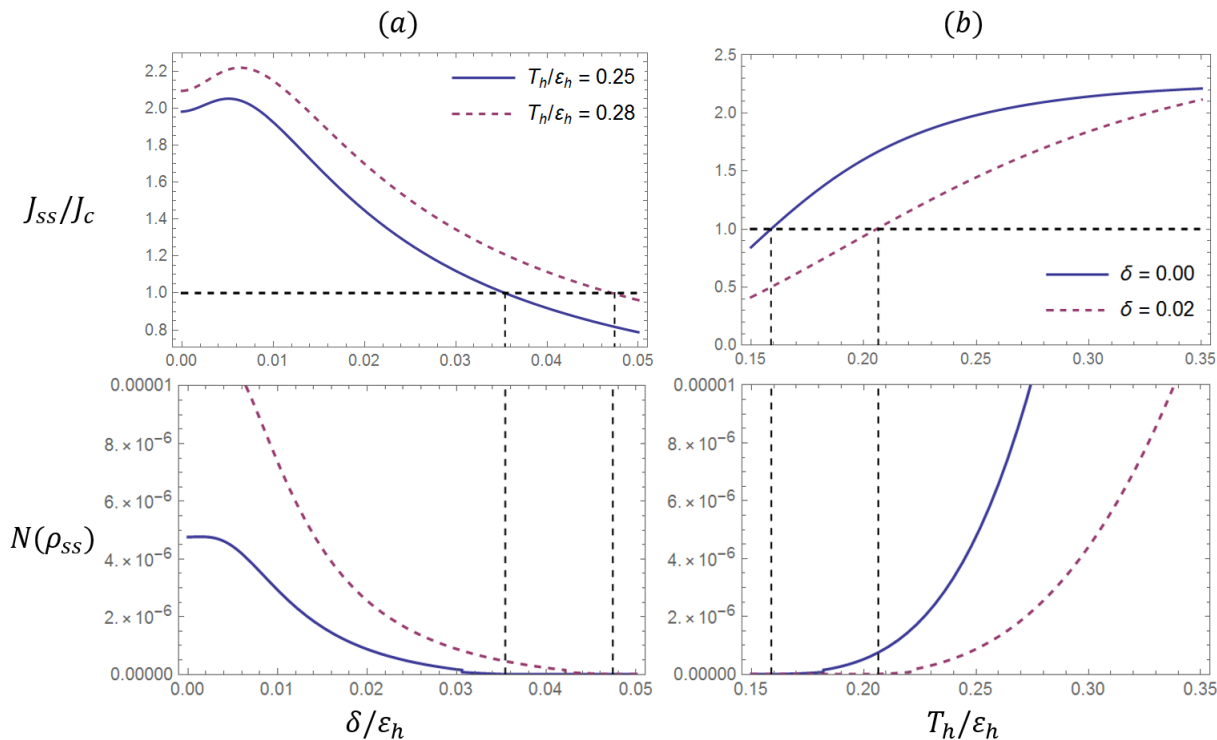


Figure 3: J_{ss}/J_c and the negativity, $N(\rho_{ss})$ as functions of (a) δ/ε_h for constant T_h/ε_h , and (b) T_h/ε_h for constant δ/ε_h . $T_c/\varepsilon_h = 0.1$, $g = 1.6 \times 10^{-3}$, $\gamma_h = 10^{-3}$ and $\gamma_c = 1.1 \times 10^{-2}$. $\varepsilon_h = 1$ is set constant.

regime of small detuning. In figure 3 (b), we perform a similar analysis but with T_h instead of the detuning. In this case, there is a monotonic increase in J_{ss}/J_c . Looking at the variation of the steady-state negativity, we find a numerical lower bound on the hot bath temperature T_h to have non-zero steady-state entanglement.

5. Effect of tunnelling

In this section, we numerically analyse the effect of tunnelling terms (off-diagonal elements) in the qubit Hamiltonians on the steady-state heat current and entanglement. As we have emphasised throughout, the detuning must be small for the local master equation approach to be valid. Additionally, a small detuning in energy gaps may be present in an experiment due to a variety of factors. It is for these reasons that for our numerical analysis, we let the detuning be small (1% of the energy gap). We let the Hamiltonian of the system be

$$H_s = \sum_{j \in \{h,c\}} \left(\varepsilon_j \sigma_+^{(j)} \sigma_-^{(j)} + \kappa_j \sigma_x^{(j)} \right) + g \left(\sigma_+^{(h)} \sigma_-^{(c)} + \sigma_-^{(h)} \sigma_+^{(c)} \right). \quad (19)$$

In figure 4, we show the variation of the steady-state heat current and negativity, with the tunnelling rate in the hot qubit, κ_h . Clearly, for smaller magnitudes, the

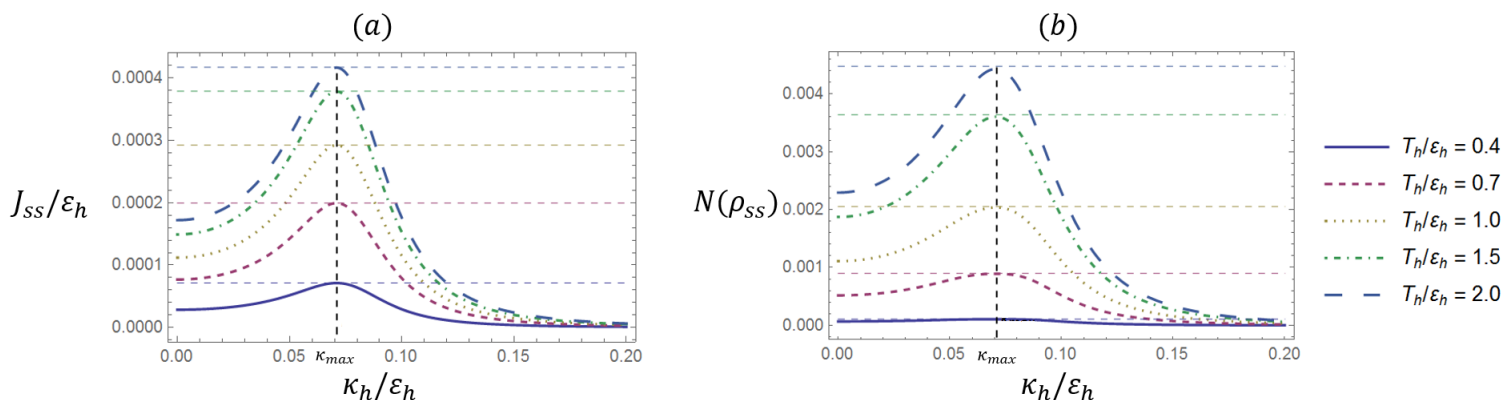


Figure 4: Steady-state heat current J_{ss}/ε_h and negativity $N(\rho_{ss})$ as functions of κ_h/ε_h , with $\kappa_c = 0$ and $\delta/\varepsilon_h = 0.01$. The horizontal dashed curves mark the heat current and negativity respectively, for $\delta = 0$ and $\kappa_h = \kappa_c = 0$, for different values of T_h/ε_h . $T_c/\varepsilon_h = 0.1$, $g = 1.6 \times 10^{-3}$, $\gamma_h = 10^{-3}$ and $\gamma_c = 1.1 \times 10^{-2}$.

effect of κ_h is to counter the effect of detuning; there is an increase in heat current as well as entanglement in the steady-state, with increasing κ_h . At a certain value of tunnelling rate κ_{max} , a maximum value of heat current and entanglement is reached, beyond which the two monotonically decrease. We find that for $\kappa = \kappa_{max}$, the heat current and entanglement are recovered, according to the numerics. The reason behind this recovery is the tunnelling term counterbalancing the effect of having off-resonant qubits. Interestingly, this maximising value κ_{max} is approximately the same for both heat current and entanglement. Furthermore, there is little variation in κ_{max} with the temperature T_h .

In figure 5, we show the behaviour of steady-state heat current and entanglement respectively with κ_1 and the detuning δ . The bright region shows the variation of κ_{max} with the detuning. We observe a non-linear but monotonic increase in κ_{max} , i.e. larger the detuning, greater the magnitude of tunnelling required to recover the heat current and entanglement. The plots show that the two-qubit thermal machine works as an entanglement engine for a large range of parameters, not only restricted to the optimised setting (energy degenerate qubits, no tunneling) considered in [14].

6. Conclusions

We provided a thorough investigation of the two-qubit thermal machine under a general condition of energy non-degeneracy and the presence of tunnelling. To obtain a steady-state solution for the system, we operated under a local Lindblad master equation approach for which it was imperative to impose restrictions of both weak coupling between qubits and small detuning. We then used the steady-state solution to study the flow of heat across the system as well as entanglement generation.

Importantly, we established an analytical relation between the heat current and

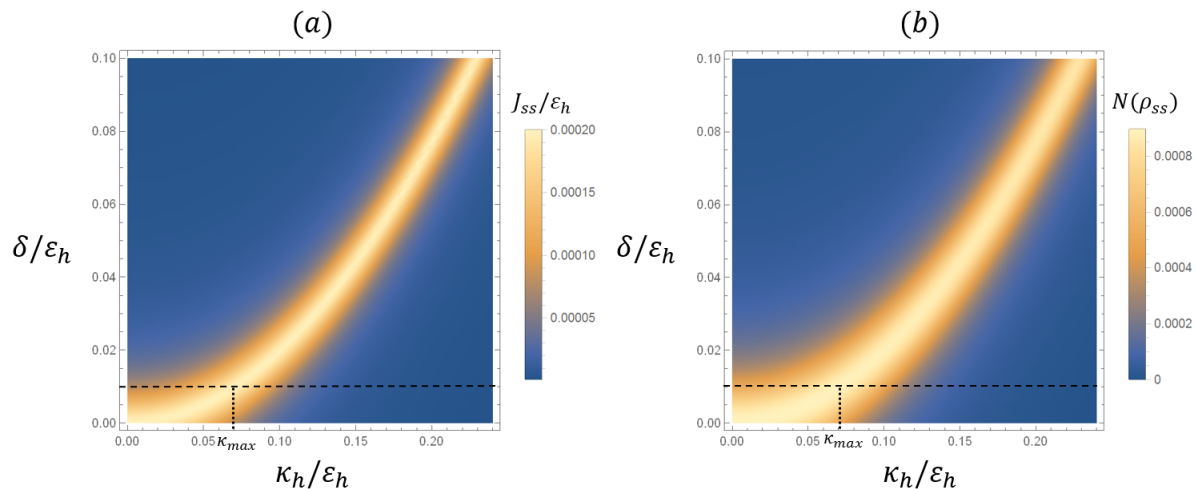


Figure 5: Steady-state (a) heat current J_{ss}/ε_h and (b) negativity $N(\rho_{ss})$ as functions of κ_h/ε_h and δ/ε_h , with $\kappa_c = 0$, $T_h/\varepsilon_h = 0.7$, $T_c/\varepsilon_h = 0.1$, $g = 1.6 \times 10^{-3}$, $\gamma_h = 10^{-3}$ and $\gamma_c = 1.1 \times 10^{-2}$. $\varepsilon_h = 1$ is set constant. The horizontal dashed lines are representative of the curves corresponding to $T_h/\varepsilon_h = 0.7$ in figure 4.

entanglement generation for our model, through the critical heat current presented in section 4.1. The two-qubit thermal machine only works successfully as an entanglement engine if the temperature gradient is sufficient and the cold bath is at a rather low temperature, as observed in [14]. This behaviour can now be fully understood by the critical heat current. In addition, we demonstrated that the bound on heat current allows one to determine precise bounds on quantities such as coupling and detuning, in order to see entanglement in the steady-state, i.e to have a working entanglement engine. From a fundamental perspective, the lower bound relates the purely quantum notion of entanglement to the flow of heat, which has its roots in classical physics.

Additionally, we presented analytical and numerical results to study the effect of detuning on steady-state heat current and entanglement. Considering the presence of a small detuning and found a reduction in both the quantities. In the presence of a tunnelling rate within one of the qubits, however, we found that the lost heat current and entanglement can be recovered. Detuning and tunnelling, being experimentally relevant parameters, this trade-off holds significance for any future implementations.

In this work, we operated exclusively in the steady-state regime. It has been earlier shown [50,51] that the transient regime can be advantageous for reaching a larger amount of entanglement. Hence, an open question concerns the behaviour of the critical current in the transient case. Furthermore, it would also be of interest to go beyond the two-qubit model to multipartite engines [29], to see how heat flow affects entanglement generation.

Acknowledgements

We acknowledge support from the Swiss National Science Foundation through the starting grant PRIMA PR00P2_179748, the grant 200021_169002, and through the NCCR QSIT - Quantum Science and Technology.

References

- [1] Kosloff R and Levy A 2014 *Ann. Rev. Phys. Chem.* **65** 365–393 URL <https://www.annualreviews.org/doi/abs/10.1146/annurev-physchem-040513-103724>
- [2] Mitchison M T and Potts P P 2018 Physical Implementations of Quantum Absorption Refrigerators *Thermodynamics in the Quantum Regime* (Springer, Cham) chap 6, pp 149–174 URL https://link.springer.com/chapter/10.1007/978-3-319-99046-0_6
- [3] Mitchison M T 2019 *Contemp. Phys.* **60** 164–187 URL <https://www.tandfonline.com/doi/full/10.1080/00107514.2019.1631555>
- [4] Linden N, Popescu S and Skrzypczyk P 2010 *Phys. Rev. Lett.* **105** 130401 URL <https://journals.aps.org/prl/abstract/10.1103/PhysRevLett.105.130401>
- [5] Levy A and Kosloff R 2012 *Phys. Rev. Lett.* **108** 070604 URL <https://journals.aps.org/prl/abstract/10.1103/PhysRevLett.108.070604>
- [6] Brunner N, Linden N, Popescu S and Skrzypczyk P 2012 *Phys. Rev. E* **85** 051117 URL <https://journals.aps.org/pre/abstract/10.1103/PhysRevE.85.051117>
- [7] Roulet A, Nimmrichter S, Arrazola J M, Seah S and Scarani V 2017 *Phys. Rev. E* **95** 062131 URL <https://journals.aps.org/pre/abstract/10.1103/PhysRevE.95.062131>
- [8] Hofer P P, Brask J B, Perarnau-Llobet M and Brunner N 2017 *Phys. Rev. Lett.* **119** 090603 URL <https://journals.aps.org/prl/abstract/10.1103/PhysRevLett.119.090603>
- [9] Erker P, Mitchison M T, Silva R, Woods M P, Brunner N and Huber M 2017 *Phys. Rev. X* **7** 031022 URL <http://link.aps.org/doi/10.1103/PhysRevX.7.031022>
- [10] Brunner N, Huber M, Linden N, Popescu S, Silva R and Skrzypczyk P 2014 *Phys. Rev. E* **89** URL <https://journals.aps.org/pre/abstract/10.1103/PhysRevE.89.032115>
- [11] Maslennikov G, Ding S, Hablützel R, Gan J, Roulet A, Nimmrichter S, Dai J, Scarani V and Matuskevich D 2019 *Nat. Commun.* **10** 202 URL <https://www.nature.com/articles/s41467-018-08090-0#citeas>
- [12] Mari A and Eisert J 2012 *Phys. Rev. Lett.* **108** 120602 URL <https://journals.aps.org/prl/abstract/10.1103/PhysRevLett.108.120602>
- [13] Venturelli D, Fazio R and Giovannetti V 2013 *Phys. Rev. Lett.* **110** 256801 URL <https://journals.aps.org/prl/abstract/10.1103/PhysRevLett.110.256801>
- [14] Bohr Brask J, Haack G, Brunner N and Huber M 2015 *New J. Phys.* **17** 113029 URL <https://iopscience.iop.org/article/10.1088/1367-2630/17/11/113029>
- [15] Hofer P P, Perarnau-Llobet M, Brask J B, Silva R, Huber M and Brunner N 2016 *Phys. Rev. B* **94** 235420 URL <https://journals.aps.org/prb/abstract/10.1103/PhysRevB.94.235420>
- [16] Hofer P P, Souquet J R and Clerk A A 2016 *Phys. Rev. B* **93** 041418 URL <https://journals.aps.org/prb/abstract/10.1103/PhysRevB.93.041418>
- [17] Mitchison M T, Huber M, Prior J, Woods M P and Plenio M B 2016 *Quant. Sci. Tech.* **1** 15001 URL <https://iopscience.iop.org/article/10.1088/2058-9565/1/1/015001/meta>
- [18] Josefsson M, Svilans A, Burke A M, Hoffmann E A, Fahlvik S, Thelander C, Leijnse M and Linke H 2018 *Nat. Nanotech.* **13** 920–924 URL <https://www.nature.com/articles/s41565-018-0200-5>
- [19] Samuelsson P, Kheradsoud S and Sothmann B 2017 *Phys. Rev. Lett.* **118** 256801 URL <https://journals.aps.org/prl/abstract/10.1103/PhysRevLett.118.256801>

- [20] Haack G and Giazotto F 2019 *Phys. Rev. B* **100** 235442 URL <https://journals.aps.org/prb/abstract/10.1103/PhysRevB.100.235442>
- [21] Chiaracane C, Mitchison M T, Purkayastha A, Haack G and Goold J 2020 *Phys. Rev. Res.* **2** 013093 URL <https://journals.aps.org/prresearch/abstract/10.1103/PhysRevResearch.2.013093>
- [22] Doyeux P, Leggio B, Messina R and Antezza M 2016 *Phys. Rev. E* **93** 022134 URL <https://journals.aps.org/pre/abstract/10.1103/PhysRevE.93.022134>
- [23] Latune C L, Sinayskiy I and Petruccione F 2019 *Sci. Rep.* **9** 3191 URL <https://www.nature.com/articles/s41598-019-39300-4>
- [24] Sánchez R, Sothmann B and Jordan A N 2015 *Phys. Rev. Lett.* **114** 146801 URL <https://journals.aps.org/prl/abstract/10.1103/PhysRevLett.114.146801>
- [25] Sánchez R, Sothmann B and Jordan A N 2015 *New J. Phys.* **17** 075006 URL <https://iopscience.iop.org/article/10.1088/1367-2630/17/7/075006/meta>
- [26] Roura-Bas P, Arrachea L and Fradkin E 2018 *Phys. Rev. B* **98** 195429 URL <https://journals.aps.org/prb/abstract/10.1103/PhysRevB.98.195429>
- [27] Gresta D, Real M and Arrachea L 2019 *Phys. Rev. Lett.* **123** 186801 URL <https://journals.aps.org/prl/abstract/10.1103/PhysRevLett.123.186801>
- [28] Tavakoli A, Haack G, Huber M, Brunner N and Brask J B 2018 *Quantum* **2** 73 URL <https://quantum-journal.org/papers/q-2018-06-13-73/>
- [29] Tavakoli A, Haack G, Brunner N and Brask J B 2020 *Phys. Rev. A* **101** 012315 URL <https://link.aps.org/doi/10.1103/PhysRevA.101.012315>
- [30] Tacchino F, Auffèves A, Santos M F and Gerace D 2018 *Phys. Rev. Lett.* **120** 063604 URL <https://link.aps.org/doi/10.1103/PhysRevLett.120.063604>
- [31] Goold J, Huber M, Riera A, Del Rio L and Skrzypczyk P 2016 *J. Phys. A* **49** 14 URL <https://iopscience.iop.org/article/10.1088/1751-8113/49/14/143001/meta>
- [32] Ordóñez-Miranda J, Ezzahri Y and Joulain K 2017 *Phys. Rev. E* **95** 022128 URL <https://journals.aps.org/pre/abstract/10.1103/PhysRevE.95.022128>
- [33] Kargi C, Naseem M T, Opatrný T, Müstecaplıoğlu Ö E and Kurizki G 2019 *Phys. Rev. E* **99** 042121 URL <https://journals.aps.org/pre/abstract/10.1103/PhysRevE.99.042121>
- [34] Breuer H P and Petruccione F 2007 *The Theory of Open Quantum Systems* vol 1 (Oxford University Press)
- [35] Schaller G 2014 *Open Quantum Systems Far from Equilibrium* (Springer, Cham)
- [36] Potts P P 2019 URL <http://arxiv.org/abs/1906.07439>
- [37] Hofer P P, Perarnau-Llobet M, Miranda L D M, Haack G, Silva R, Brask J B and Brunner N 2017 *New J. Phys.* **19** 123037 URL <https://iopscience.iop.org/article/10.1088/1367-2630/aa964f>
- [38] Onam González J, Correa L A, Nocerino G, Palao J P, Alonso D and Adesso G 2017 *Open Sys. Inf. Dyn.* **24** 1740010 URL <https://www.worldscientific.com/doi/abs/10.1142/S1230161217400108>
- [39] Mitchison M T and Plenio M B 2018 *New J. Phys.* **20** 033005 URL <https://iopscience.iop.org/article/10.1088/1367-2630/aa9f70>
- [40] Alicki R 1979 *J. Phys. A* **12** 5 URL <https://iopscience.iop.org/article/10.1088/0305-4470/12/5/007/meta>
- [41] Alicki R and Kosloff R 2018 Introduction to Quantum Thermodynamics: History and Prospects *Thermodynamics in the Quantum Regime* ed Binder F, Correa L A, Gogolin C, Anders J and Adesso G (Springer, Cham) pp 1–33 URL https://link.springer.com/chapter/10.1007/978-3-319-99046-0_{_}1
- [42] Moskalets M and Büttiker M 2004 *Phys. Rev. B* **70** 245305 URL <https://journals.aps.org/prb/abstract/10.1103/PhysRevB.70.245305>
- [43] Lesovik G B and Sadovskyy I A 2011 *Phys.-Uspekhi* **54** 1007 URL <https://iopscience.iop.org/article/10.3367/UFNe.0181.201110b.1041>
- [44] Rego L G and Kirczenow G 1998 *Phys. Rev. Lett.* **81** 232 URL <https://journals.aps.org/prl/abstract/10.1103/PhysRevLett.81.232>

- [45] Segal D and Nitzan A 2005 *Phys. Rev. Lett.* **94** 034301 URL <https://link.aps.org/doi/10.1103/PhysRevLett.94.034301>
- [46] Życzkowski K, Horodecki P, Sanpera A and Lewenstein M 1998 *Phys. Rev. A* **58** 883–892 URL <https://link.aps.org/doi/10.1103/PhysRevA.58.883>
- [47] Vidal G and Werner R F 2002 *Phys. Rev. A* **65** 032314 URL <https://journals.aps.org/pr/abstract/10.1103/PhysRevA.65.032314>
- [48] Peres A 1996 *Phys. Rev. Lett.* **77** 1413–1415 URL <https://journals.aps.org/prl/abstract/10.1103/PhysRevLett.77.1413>
- [49] Horodecki M, Horodecki P and Horodecki R 1996 *Phys. Lett. A* **223:1-2** 1–8 URL <https://www.sciencedirect.com/science/article/pii/S0375960196007062>
- [50] Brask J B and Brunner N 2015 *Phys. Rev. E* **92** 062101 URL <https://journals.aps.org/pre/abstract/10.1103/PhysRevE.92.062101>
- [51] Mitchison M T, Woods M P, Prior J and Huber M 2015 *New J. Phys.* **17** 115013 URL <https://iopscience.iop.org/article/10.1088/1367-2630/17/11/115013>

Appendices

A. Steady-state solution

To obtain the steady-state solution in section 2, we recast (3) as a matrix differential equation for the vectorised state $\mathbf{p}(t)$ of the density operator $\rho(t)$.

$$\rho(t) \longleftrightarrow \mathbf{p}(t), \quad \dot{\rho}(t) = \mathcal{L}\rho(t) \longleftrightarrow \dot{\mathbf{p}}(t) = M\mathbf{p}(t) + \mathbf{b} \quad (20)$$

M is a 15×16 matrix, and \mathbf{p} and \mathbf{b} are 15×1 vectors (one element of \mathbf{p} can be eliminated using $\text{Tr}(\rho(t)) = 1$), which are explicitly given by

$$M =$$

$$\begin{pmatrix} -\gamma_h^- - \gamma_c^- & 0 & 0 & 0 & 0 & \gamma_c^+ & 0 & 0 & 0 & 0 & \gamma_h^+ & 0 & 0 & 0 & 0 \\ 0 & \frac{1}{2}(-2\gamma_h^- - \Gamma_c) - i\varepsilon_c & ig & 0 & 0 & 0 & 0 & 0 & 0 & 0 & 0 & \gamma_h^+ & 0 & 0 & 0 \\ 0 & ig & \frac{1}{2}(-\Gamma_h - 2\gamma_c^-) - i\varepsilon_h & 0 & 0 & 0 & 0 & \gamma_c^+ & 0 & 0 & 0 & 0 & 0 & 0 & 0 \\ 0 & 0 & 0 & -\frac{1}{2}\Gamma - i(\varepsilon_h + \varepsilon_c) & 0 & 0 & 0 & 0 & 0 & 0 & 0 & 0 & 0 & 0 & 0 \\ 0 & 0 & 0 & 0 & \frac{1}{2}(-2\gamma_h^- - \Gamma_c) + i\varepsilon_c & 0 & 0 & 0 & -ig & 0 & 0 & 0 & 0 & 0 & \gamma_h^+ \\ \gamma_c^- - \gamma_h^+ & 0 & 0 & 0 & 0 & -\Gamma_h - \gamma_c^+ & ig & 0 & 0 & -ig & -\gamma_h^- & 0 & 0 & 0 & 0 \\ 0 & 0 & 0 & 0 & 0 & ig & -\frac{1}{2}\Gamma + i\delta & 0 & 0 & 0 & -ig & 0 & 0 & 0 & 0 \\ 0 & 0 & 0 & 0 & 0 & 0 & 0 & \frac{1}{2}(-\Gamma_h - 2\gamma_c^+) - i\varepsilon_h & 0 & 0 & 0 & -ig & 0 & 0 & 0 \\ 0 & 0 & 0 & 0 & 0 & 0 & 0 & 0 & 0 & \frac{1}{2}(-\Gamma_h - 2\gamma_c^-) + i\varepsilon_h & 0 & 0 & 0 & 0 & \gamma_c^+ \\ 0 & 0 & 0 & 0 & 0 & -ig & 0 & 0 & 0 & 0 & 0 & 0 & 0 & 0 & 0 \\ \gamma_h^- - \gamma_c^+ & 0 & 0 & 0 & 0 & -ig & 0 & 0 & 0 & -\frac{1}{2}\Gamma - i\delta & ig & 0 & 0 & 0 & 0 \\ 0 & \gamma_h^- & 0 & 0 & 0 & 0 & -ig & 0 & 0 & ig & -\gamma_h^+ - \Gamma_c & 0 & 0 & 0 & 0 \\ 0 & 0 & 0 & 0 & 0 & 0 & 0 & -ig & 0 & 0 & 0 & \frac{1}{2}(-2\gamma_h^- - \Gamma_c) - i\varepsilon_c & 0 & 0 & 0 \\ 0 & 0 & 0 & 0 & 0 & 0 & 0 & 0 & 0 & 0 & 0 & 0 & -\frac{1}{2}\Gamma + i(\varepsilon_h + \varepsilon_c) & 0 & 0 \\ 0 & 0 & 0 & 0 & 0 & 0 & 0 & 0 & 0 & 0 & 0 & 0 & 0 & \frac{1}{2}(-\Gamma_h - 2\gamma_c^+) + i\varepsilon_h & 0 \\ 0 & 0 & 0 & 0 & 0 & 0 & 0 & 0 & \gamma_c^- & 0 & 0 & 0 & 0 & ig & \frac{1}{2}(-2\gamma_h^- - \Gamma_c) + i\varepsilon_c \\ 0 & 0 & 0 & 0 & 0 & \gamma_h^- & 0 & 0 & 0 & 0 & 0 & 0 & 0 & 0 & ig \end{pmatrix} \quad (21)$$

and

$$\mathbf{b} = (0, 0, 0, 0, 0, \gamma_h^+, 0, 0, 0, 0, \gamma_c^+, 0, 0, 0, 0)^T. \quad (22)$$

The steady-state solution is simply given by $\mathbf{p}_{\text{ss}} = -M^{-1}\mathbf{b}$.

B. Steady-state negativity

We know that the form of the interaction Hamiltonian H_{int} imposes that the steady-state of the two qubits takes the form given by (6). The eigenvalues λ_j of its partial

transpose are listed below.

$$\begin{aligned} \lambda_1 = r_2 & & \lambda_3 = \frac{1}{2} \left(-\sqrt{4|c|^2 + (r_1 - r_4)^2} + r_1 + r_4 \right) \\ \lambda_2 = r_3 & & \lambda_4 = \frac{1}{2} \left(\sqrt{4|c|^2 + (r_1 - r_4)^2} + r_1 + r_4 \right) \end{aligned} \quad (23)$$

Since only λ_3 can take a negative value, the steady-state negativity is simply given by

$$N(\rho_{\text{ss}}) = \max \{0, -\lambda_3\}. \quad (24)$$